View metadata, citation and similar papers at core.ac.uk

brought to you by CORE

provided by Open Archive Toulouse Archive Ouverte

Open Archive Toulouse Archive Ouverte (OATAO)

OATAO is an open access repository that collects the work of some Toulouse researchers and makes it freely available over the web where possible.

This is an author's version published in: http://oatao.univ-toulouse.fr/20585

Official URL: https://doi.org/10.1016/j.cej.2015.04.108

To cite this version:

Ali, Aamer and Aimar, Pierre and Drioli, E. Effect of module design and flow patterns on performance of membrane distillation process. (2015) Chemical Engineering Journal, 277. 368-377. ISSN 1385-8947

Any correspondence concerning this service should be sent to the repository administrator:

tech-oatao@listes-diff.inp-toulouse.fr

Effect of module design and flow patterns on performance of membrane distillation process

A. Ali [b,d,*], P. Aimar [d,f,1], E. Drioli [a,b,c,e,2]

[a] National Research Council – Institute on Membrane Technology (ITM–CNR), Via Pietro BUCCI, c/o The University of Calabria, cubo 17C, 87036 Rende, CS, Italy
[b] The University of Calabria – Department of Chemical Engineering and Materials, cubo 44A, Via Pietro BUCCI, 87036 Rende, CS, Italy
[c] Hanyang University, WCU Energy Engineering Department, Room 917 9th Floor FTC Bldg., 17 Haengdang-dong, Seongdong-gu, Seoul 133-791, South Korea
[d] Université de Toulouse; INPT, UPS; Laboratoire de Génie Chimique; 118 Route de Narbonne, F-31062 Toulouse, France
[e] KAU – CEDT, Jeddah, Saudi Arabia
[f] CNRS; Laboratoire de Génie Chimique; F-31062 Toulouse, France

HIGHLIGHTS

- Effect of fiber configurations and flow patterns on MD performance has been studied.
- Undulating fibers show best performance in terms of flux at low feed flow rates.
- Helical modules and intermittent flows exhibit better energy efficiency.
- Intermittent and pulsatile flows are the best optimum.

Keywords:
Hollow fiber configurations
Flow patterns
Membrane distillation
Energy efficiency
Packing density
Enhancement factors

ABSTRACT

The present study highlights the effect of different hollow fiber membrane configurations and flow patterns on performance of membrane distillation (MD) process. The modules with helical and wavy conformations have been tested under various hydrodynamic conditions and their performance has been compared with conventional straight fiber modules. The effect of flow patterns has been studied by applying the intermittent and pulsating flows to straight hollow fiber membranes. A flux enhancement of 47% and 52% with respect to the straight fibers has been observed for helical and wavy configurations, respectively, though packing density of such modules is significantly less than their straight counterparts. For intermittent flow, an improvement of ~30% has been recorded. The difference is more prominent at low flow rates and approaches to the straight fiber performance under steady flow at high Reynolds numbers (*Re*) for all hollow fiber configurations and flow patterns studied. The intermittent flow and wavy fibers exhibit an energy efficiency enhancement of ~180% and ~90% over their conventional counter parts, respectively. In terms of surface and volume based enhancement factor and packing density, intermittent and pulsating flow exhibited the most optimal performance.

1. Introduction

Membrane distillation (MD) is an emerging process based on temperature gradient created across a microporous hydrophobic membrane that allows the passage of vapors only, thus retaining theoretically all non-volatiles present in the feed. The process provides the opportunity to concentrate the solution to their saturation level and the possibility to use waste grade energy. MD as standalone process or in integration with other processes finds interesting potential applications in numerous fields including desalination, wastewater treatment, recovery of minerals from various effluents, semiconductor industry, dairy sector, etc. [1]. Traditionally, MD has been operated in four well known configurations including direct contact membrane distillation (DCMD), vacuum membrane distillation (VMD), sweep gas membrane distillation (SGMD) and air gap membrane distillation (AGMD). Some new configurations have also been introduced recently [2–4].

Energy intensive nature and limited flux are the major obstacles in successful and widespread commercial adoption of MD. A

* Corresponding author at: National Research Council – Institute on Membrane Technology (ITM–CNR), Via Pietro BUCCI, c/o The University of Calabria, cubo 17C, 87036 Rende, CS, Italy. Tel.: +39 38 90020234.
E-mail addresses: amir_hmmad@hotmail.com, aamer.ali@vscht.cz (A. Ali), Pierre.Aimar@univ-toulouse.fr (P. Aimar), e.drioli@itm.cnr.it (E. Drioli).
[1] Tel.: +33 5 61 55 83 04.
[2] Tel.: +39 0984492039.

http://dx.doi.org/10.1016/j.cej.2015.04.108

significant amount of heat is dissipated in the process due to temperature or thermal polarization characterized by the difference in temperatures at the membrane surfaces and in bulk phases [5]. Among all the configurations, thermal polarization is the worst in DCMD which is the most studied configuration of MD. The effect of temperature polarization on flux reduction in membrane distillation has been well acknowledged in numerous investigations [6–8]. In addition to thermal polarization, surface scaling and organic fouling have also been found to depreciate MD performance as observed in various studies [9–12]. Hydrophobic nature of the membranes used makes it more susceptible to organic fouling. Under high convective flux, concentration polarization can also play significant role in limiting the flux of the process.

In order to mitigate thermal polarization, scaling/fouling and possible concentration polarization, MD can benefit from the solutions developed by the process industry to tackle the similar problems in other processes. For instance, most of the conventional techniques applied for fouling and concentration polarization reduction in pressure driven membrane processes [13] may provide interesting solution to mitigate thermal and concentration polarization in MD. However, due to limited flux (and therefore products), the techniques that consume too much energy may not be suitable for MD. After considering these factors, the most interesting techniques for MD are limited to only a few candidates. A pros and cons analysis of different state-of-the-art hydraulic techniques practiced for conventional membrane processes with application potential for MD has been provided in Table 1. Most of these techniques cannot only reduce the fouling in MD but they can also improve temperature distribution within the membrane module. The techniques can also have "wash away" effect on surface scales/crystals.

As pointed out in Table 1, one potentially feasible passive approach for improving heat transfer and reducing fouling in MD can be based on induction of the secondary flows inside the hollow fibers. The generation of secondary flows can be conveniently realized by using the undulating geometries. When a fluid flows in such channels, the centrifugal force caused by the geometry of the channel forces the fluid to flow toward the outer wall, thus creating a secondary flow or counter rotating vortices also referred as Dean Vortices. The phenomenon was first studied systematically by Dean [27] and was applied to pressure driven membrane operations by some groups later on. A good review of the concept as applied to the membrane processes can be found in reference [28]. Helically coiled membrane modules have been effectively used to create such vortices inside the hollow fiber membranes to reduce the fouling in pressure driven processes [29–32]. The secondary flows direct the foulants away from the membrane surface. The same concept has been used to increase heat transfer coefficient in heat exchangers [33–35]. The approach can be very promising for membrane distillation to improve the temperature polarization coefficient of the process both at upstream and downstream and to reduce the fouling and concentration polarization. Similar to helical geometries, crimped or wavy fibers have been used in membrane contactor and heat exchanger applications to increase mass and heat transfer coefficients [36–38]. Fundamental introduction to use of similar geometries for MD applications has been studied recently [17]. These geometries, however, reduce the packing densities of the fibers. Therefore, energy efficiency, area based enhancement factor (increase in flux per unit change in surface area) and volume based enhancement factor (increase in flux per unit change in module volume) should be introduce to comprehend the performance of such geometries.

The use of active techniques including ultrasonic stimulation and air bubbling has also been found affective in elevating the performance of MD [39,40,21]. Another interesting active approach to reduce concentration and thermal polarization can be realized by changing the flow pattern of the fluid flowing in a channel. Intermittent flow and pulsating flow are two common approaches used to realize this objective. The use of intermittent flow has been proven effective in increasing heat and mass transfer for separation and heat transfer applications [41,42]. On the other hand, pulsating flow has gained more attention for medical and biological applications [18,43]. Some studies have shown an improved heat transfer for pulsating flow [44–46]. Moreover, significantly improvement in performance of ultrafiltration has been claimed in another investigation [20].

Despite the use of various membrane configurations and flow patterns mentioned in above paragraphs for conventional pressure driven processes, the use of such approaches for MD applications has not been well explored. Current study aims to investigate the effect of secondary flows and flow patterns on performance of direct contact membrane distillation process. Induction of secondary flows has been realized by using helical and wavy shaped fibers under different hydrodynamic conditions. The pulsating and intermittent flows have been generated by using simple mechanical modifications of the conventional set-up used for MD. A comparative analysis of both approaches in terms of flux enhancement, energy efficiency, area base enhancement factor and packing density has also been provided.

Table 1
A brief analysis of possible hydraulic techniques for fouling and thermal polarization reduction in MD.

Technique	Potential benefits	Potential challenges	Selected references
Induction of secondary flow	No extra equipment required, easy to adopt, strong effect on temperature polarization on up and down stream sides, high shear acting on the surface can remove the attached particles and fouling layer built up, the performance can be tuned simply by changing the coil diameter and pitch.	Although for heat exchangers and low pressure membrane processes, the process has been well studied yet further studies are required to establish the effects for MD	[14–17]
Pulsating and intermittent flows	Reduction in concentration and thermal polarization, relatively simple to incorporate	Additional operational and capital cost associated with the flow patterns generating equipment	[18–20]
Air sparging	Reduction in fouling and thermal polarization	Additional cost related with air sparging equipment, air can occupy the part of membrane modules thus reducing the contacting area, the pores can be occupied by the injected air leading towards reduced vapor pressure	[21,22]
Backwashing	Removal of crystals, scales and deposits partially covering the pores	The pore wetting will occur leading to the post drying requirement, the effectiveness of the technique will be limited to remove deposition, scaling occurred within the pore or at pore mouth, no effect on thermal polarization	[23,24]
Rotating membranes	Reduction in concentration and thermal polarization	High energy consumption, design modification for MD can be complicated, may not be suitable for hollow fibers	[25,26]

2. Materials and methods

2.1. Membrane applied

The membrane used in the experimentation was a hollow fiber PP membrane (Acuurel S6/2 PP, Membrana, Germany). The membrane has internal and external diameters of 1.80 and 2.70 mm, respectively. The porosity of the membrane has been reported as 73% by the manufacturer.

2.2. Formation of helical and wavy fibers

The helical fibers used in the study were prepared by simply winding the fibers around a rod of particular diameter as shown in Fig. 1. The rod used had outer diameter of 10 mm while the pitch of hollow fiber helix was adjusted at 40 mm. The supports were provided at four different locations on the rod in order to avoid the contact of fiber with the pipe, as the contact area can reduce the flux. The wrapped fibers were enclosed in a glass module and the ends of the module were sealed so that the feed can pass only through the fibers. In parallel to the helical module, a wavy fiber module was also prepared by using the same PP membrane. The formation of wavy fiber was realized by heat treatment of the twisted fibers. After knitting the fibers in wave type pattern, the heat treatment process was carried out in an oven at a temperature of 80 °C for 30 min. The heat treatment sets the membranes in their knitted configuration even after removing the knitting supports. Wave length and amplitude of the fiber were set at 40 and 5 mm, respectively. A further decrease in wave length at this amplitude was not possible due to rigidity of the membrane. The fibers were assembled in glass modules for further testing.

2.3. Induction of intermittent and pulsating flow

Operational principle of peristaltic pump is based upon the compression and relaxation of a flexible tube positioned between rotating elements (generally rollers) and circular pump housing. Due to their rotation, fluid present ahead of rollers is pushed forward while relaxation of portion of the flexible tube just behind the roller recovers its original shape to create a vacuum that draws the fluid into the tube. However if some of the rollers are removed, the vacuum created can draw some liquid back which was initially pushed forward, thus creating a back and forth flow. The relative magnitude of forward and backward components can be controlled by adjusting the frequency through rotational speed of the pump. At very low rotational speeds, both flow components are equal and no net flow is observed. With further increase in rotational speed, the effect of forward component prevails and an intermittent flow at the tube outlet is observed. The magnitude of this flow is the net of backward and forward component of back and forth flow pattern. The scheme of intermittent flow developed in current study according to the procedure explained has been illustrated in Fig. 2. A simple arrangement was used to create the pulsating flow in the current study by applying two pumps: the steady component of pulsating flow was generated by using a rotary pump that delivers a constant flow while unsteady or intermittent component was obtained according to the procedure described above. Both these flows were combined at the module inlet to get the exact pulsating flow according to the scheme illustrated in Fig. 3. *Re* and corresponding frequency for pulsating flow was changed by changing the flow rate of intermittent component while keeping the steady component at a fixed value.

2.4. MD tests

MD tests were performed at different feed flow rates and at fixed feed temperature of 54 ± 0.3 °C, except in one case where the experimentation was performed at 45 °C to test the behavior of helical and straight fiber modules under the conditions of low thermal polarization. In all cases, permeate temperature and flow rate were set at 20 °C and 100 ml/min, respectively. Feed flow rates along with the other module characteristics have been provided in Table 2. The performance of helical module was also tested against whey solution with 10% (w/w) initial composition. Whey solution was selected due to recently emerging interest for MD in dairy industry [12,47]. Each liter of whey solution contained 8.16 g ashes, 6.11 g B lactoglobulin, 1.39 g alpha-lactalbumin, 0.48 g calcium and 0.64 g phosphorous. Feed and permeate were in countercurrent arrangement for all cases considered.

2.5. Process modeling

As the major objective of fabricated modules and flow patterns is to mitigate the thermal polarization, therefore, their performance would be more prominent under the conditions characterized by high thermal polarization. In order to establish effective and feasible ranges of heat transfer coefficients, a simple modeling was performed. Initially the membrane surface temperatures on feed and permeate sides are assumed equal to their corresponding values in the bulk phases and *Re* and Prandtl (*Pr*) numbers are calculated according to the following correlations:

$$Re = \frac{\rho v D}{\mu} \tag{1}$$

$$Pr = \frac{C_p \mu}{K} \tag{2}$$

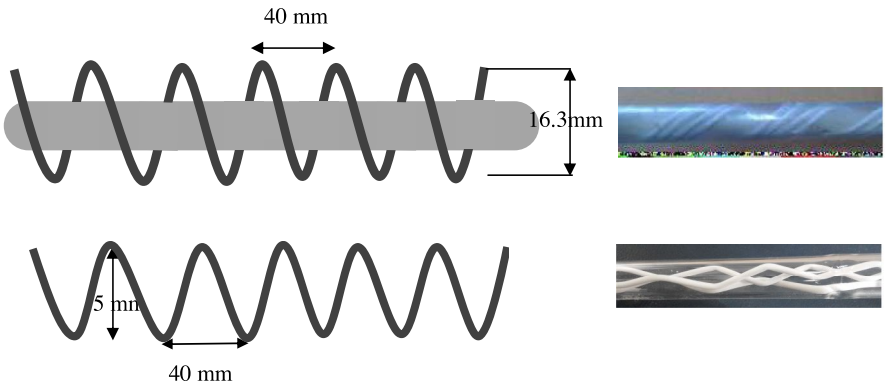

Fig. 1. Schematic diagrams and pictures of the helical and wavy modules prepared in the lab.

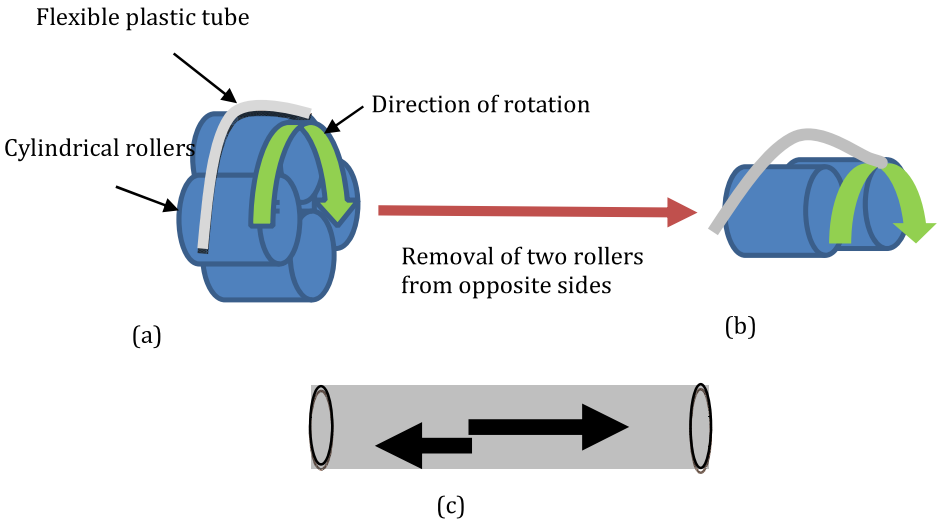

Fig. 2. Simple procedure of inducing intermittent flow through a peristaltic pump and the resultant flow pattern generated (a) Normal arrangement of cylindrical rollers present in a peristaltic pump. (b) Two opposite sided rollers have been removed to generate intermittent flow. (c) Oscillations of flow generated within the tube after removing two rollers.

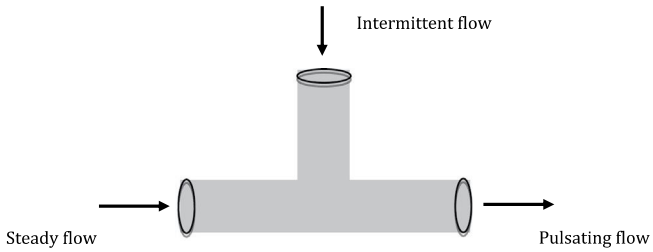

Fig. 3. A simple arrangement applied to create pulsating flow. The intermittent flow generated according to the procedure explained in Fig. 2 was combined with steady flow generated through rotary pump. Both flows from two pumps were combined at module inlet to generate the pulsating flow.

Table 2
Different module characteristics and ranges of feed flow rates used in the study.

Module type	No. of fibers	Fiber length (cm)	Membrane area (m^2)	Feed flow rate (ml/min)
Straight	4	20.1	0.00455	20–565
Helical	4	23.2	0.00524	20–240
Wavy	3	20.5	0.00348	16–138
$Straight_{IF}$	4	20.1	0.00455	10–120
$Straight_{PF}$	4	20.1	0.00455	26–100

Subscripts IF and PF represent the straight fiber module used for intermittent and pulsating flows, respectively.

Heat transfer coefficients on permeate (h_p) and feed sides (h_f) have been calculated according to different correlations provided in Table A1 given in Appendix.

Eqs. (3) and (4) have been used to calculate the temperature at membrane surfaces:

$$T_{fm} = T_f - (T_f - T_p)\frac{1/h_f}{\frac{1}{h_v+h_c}+\frac{1}{h_p}+\frac{1}{h_f}} \tag{3}$$

$$T_{pm} = T_p + (T_f - T_p)\frac{1/h_p}{\frac{1}{h_v+h_c}+\frac{1}{h_p}+\frac{1}{h_f}} \tag{4}$$

where h_c and h_v are conductive and vapor heat transfer coefficients of membrane, respectively:

$$h_v = \frac{J\Delta H_v}{T_{fm} - T_{pm}} \tag{5}$$

$$h_c = \frac{k_m}{\delta} \tag{6}$$

where H_v is the enthalpy of vapors at average membrane temperature and k_m and δ represents thermal conductivity and thickness of membrane, respectively. Temperatures predicted by Eqs. (3) and (4) have been used to recalculate Re, Pr, h_p, h_f, h_v, H_v and the corresponding temperatures at membrane surface, according to the algorithm provided in Fig. A1 given in Appendix. Iterative process is repeated till the temperatures calculated according to Eqs. (3) and (4) match with the ones used for calculation of all the relevant parameters. Temperatures predicted by various correlations and the corresponding value of membrane characteristics parameter (B) predicted by combined Knudsen and molecular diffusion model have been used to calculate theoretical flux according to Eq. (7). Selection of mass transfer model is based upon the fact that the average membrane pore size and mean free path of water vapors (~0.13 μm) within the conditions applied in the work are comparable:

$$J = B(T_{fm} - T_{pm}) \tag{7}$$

where:

$$B = \left[\frac{3\tau\delta_m}{2\varepsilon r}\left(\frac{\pi RT}{8M}\right)^{1/2} + \frac{\tau\delta_m}{\varepsilon}\frac{Pa}{PD}\frac{RT}{M}\right]^{-1} \tag{8}$$

Once the flux and interfacial temperatures are known, resistances offered by feed side boundary layer (R_f), permeate side boundary (R_p) and membrane (R_m) have been calculated according to the following expressions:

$$R_f = \frac{P_f - P_{fm}}{J} \tag{9}$$

$$R_p = \frac{P_{pm} - P_p}{J} \tag{10}$$

$$R_m = \frac{P_{fm} - P_{pm}}{J} \tag{11}$$

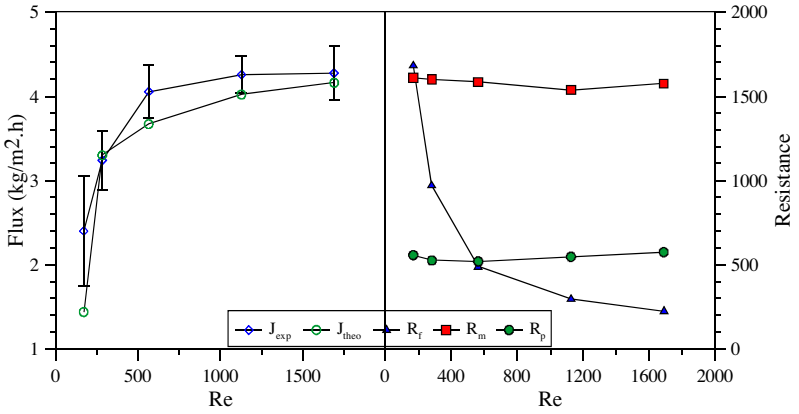

Fig. 4. Variation of experimental and theoretical flux and corresponding resistances to mass transfer as function of *Re* at average feed temperature of 54 °C.

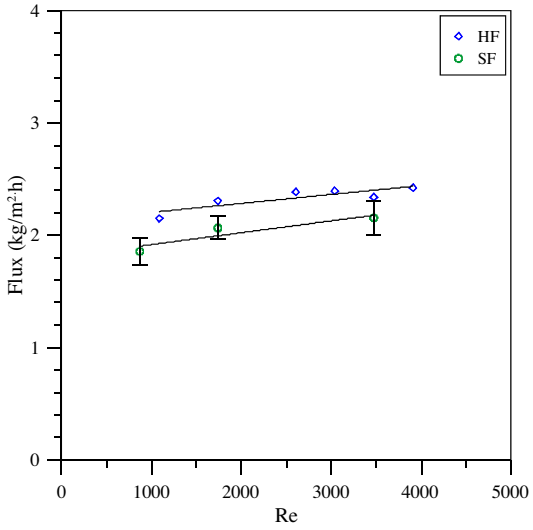

Fig. 5. Comparison of flux observed for the modules with straight (SF) and helical fibers (HF).

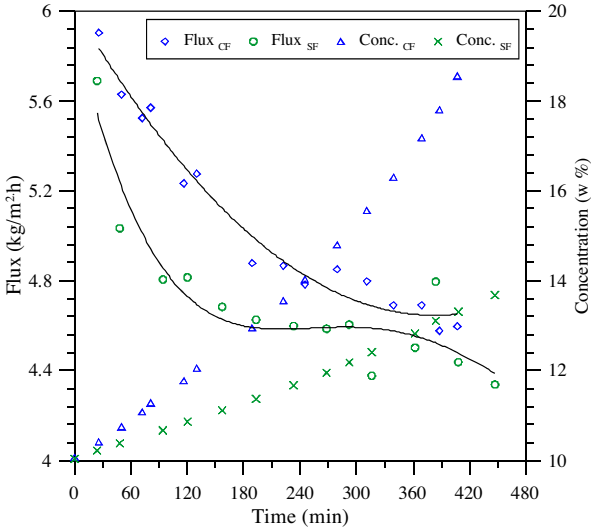

Fig. 6. Flux and concentration achieved for straight and helical coiled modules with whey solution as feed.

Energy efficiency (*EE*) is an important parameter to assess the effectiveness of utilized energy for a module. Generally, the process performance in MD is based on the energy associated with its convective and conductive components transported through the membrane. In the present study, the total energy transported through the system is calculated by applying the enthalpy balance on entrance and exit of feed stream. *EE* has been calculated by using the following expression [48]:

$$EE = \frac{J\lambda}{\frac{\dot{m} C_p \Delta T}{A_m}} \tag{12}$$

where A_m is the active membrane area through which heat transfer takes place while λ is latent heat of vaporization of water.

3. Results and discussion

3.1. Resistance analysis

Theoretical flux predicted by various heat transfer correlations calculated according to the procedure described in Section 2.5 was compared with experimental flux. The correlation (A2) was found to be the most suitable to describe the behavior of the system and was used further to calculate different resistances to mass transfer. Experimental (J_{exp}) and theoretical (J_{theo}) fluxes and corresponding various resistances to mass transfer as function of *Re* have been shown in Fig. 4. Deviation of theoretical predictions from the experimental values is in the range of experimental errors. An abrupt increase in both experimental and theoretical fluxes can be seen as *Re* increases from ~160 to ~280. It can also be inferred from the figure that values of *Re* exceeding ~550 are not significantly important in increasing the flux of this particular system. This behavior can be explained on the basis of resistance analysis shown in the same figure. The figure reveals that R_f decreases sharply by increasing feed flow rate and approaches to resistance offered by the permeate side boundary layer at *Re* ~550. It is also evident from the figure that effective reduction in R_f occurs only at low feed flow rates as at high *Re*, the major resistance to mass transfer arises from the membrane itself instead of the feed side boundary layer.

3.2. Mass flux and energy efficiency analysis

3.2.1. Helical and wavy modules

Mass flux for helical module under low thermal polarization conditions characterized by *Re* = 1086 to 3908 that corresponds to a Dean number of 339 to 1219 (calculated in accordance with [49]) and feed temperature of 45 °C has been shown in Fig. 5. It

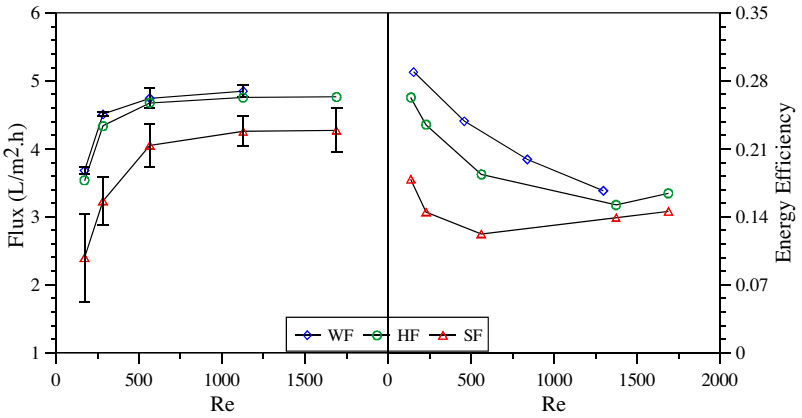

Fig. 7. Flux and energy efficiency for wavy (WF), helical fibers (HF) and straight fiber modules as function of feed side *Re*.

is clear from the figure that flux is not significantly sensitive to the flow rate. Increased feed flow rate improves temperature polarization coefficient that enhances the flux under most of the circumstances. Very marginal increase in flux can be associated with the corresponding minor increase in temperature polarization coefficient on feed side. The results are in accordance with explanation provided in Section 3.1: at high *Re*, the process is not limited by the boundary layer resistance on the feed side, rather by the resistance offered by the membrane and permeate side boundary layer. The presence of secondary flows makes the temperature homogeneous even at lower *Re* due to better mixing of the fluid present in the bulk and at the membrane surface. Therefore, similar trend has been observed for helical module too. The maximum difference observed in the flux of straight and coiled fibers is 10% which is expected to raise at lower feed flow rates. The difference in flux observed for the two configurations considered can be attributed mainly to improvement of heat transfer on permeates side boundary layer for helical modules.

The performance of helical and straight fiber was also compared by using whey solution as feed. The experimentation was carried out at feed temperature of 54 °C and feed side *Re* of ∼880. Due to its tendency to rapidly interacting with hydrophobic membrane, whey was used as the feed solution. The flux obtained and the corresponding concentrations for inside-out configuration for helical and straight fiber modules have been shown in Fig. 6. As illustrated in the figure, the flux exhibited by the coiled modules is higher than its straight counterpart throughout the experimental run.

Another interesting results obtained through the helically coiled module is the high flux even at high feed concentration. As shown in Fig. 6, the concentrations achieved with helical and straight modules are 18.6% and 13.7%, respectively. The solute present in the feed can affect the MD flux in several possible ways: by building up the fouling layer at the membrane surface that offers an additional resistance to mass and heat transfer, by lowering the vapor pressure of feed solution, by adsorbing on the membrane surface and by introducing concentration polarization if the convective flux is high. Initial high reduction in flux is consistent with the previous MD studies [50] carried out on whey solution where a rapid flux decline was observed mainly due to adhesion of certain whey components with membrane surface. Time interval (∼3 h) over which the major flux decline takes place is different in current study as compared to one mentioned in [50] perhaps due to different type of whey and membrane used. Relatively higher flux for helical module observed in current study can be associated with decreased thermal polarization and possible detachment of any component from feed solution interacting with the membrane surface.

When comparing the flux obtained through straight and coiled fiber modules, it should also be noted that residence time of the solution inside the coiled module is higher as compared to straight modules due to total length of helical fiber which is almost 15.4% more than that of the straight one. Higher residence time associated with the relatively longer dimension tends to reduce the average driving force along the helical module under the same thermal and hydrodynamic conditions applied at inlet of the two module configurations used.

In order to establish the performance of helical and wavy modules under low *Re* and relatively high feed temperature, the experimentation was carried out at *Re* ∼160–1680 at feed inlet temperature of 54 °C. The results for mass flux and corresponding energy efficiency are shown in Fig. 7 in form of flux under the same hydrodynamic and thermal conditions. At feed side *Re* of ∼160, the flux for helical fibers is ∼47% higher than straight fibers and this number decreases to ∼11% at high feed flow rate. For wavy fibers, 52% increase in flux over its straight counterpart has been observed. The increase in flux for helical and wavy fibers can be associated with improvement in thermal polarization at both feed and permeate sides. Higher difference in flux between straight and undulating configuration at low feed flow rates is a clear evidence of effectiveness of wavy and helical configuration in reducing the thermal polarization. Relative insensitiveness of the flux towards feed flow rate at high *Re* is qualitatively consistent with the results presented in Section 3.1. Similar dependence of flux on feed flow rate for such geometries has been observed in other studies as well [17,36]. The magnitude of improvement cited in those studies is relatively different from what has been observed in current investigation. The reason can be associated with different characteristics of membranes applied, module design parameters used and operating conditions applied.

A comparison of *EE* for helical and wavy modules with straight fiber modules has also been provided in Fig. 7 which indicates that *EE* for wavy modules is ∼90% higher than the module containing straight fibers at intermediate flow rates. At high feed flow rates, however, the difference in *EE* for both modules narrows down to 23%. With initial small increase in flow rate, the flux for helical fibers increases rapidly and then reaches a steady state range abruptly. At high feed flow rates, the flux does not increase significantly and overall impact reduces the *EE* of the system. Similarly for helical fiber, a maximum increase of 64% in *EE* has been observed which reduces at high flow rates.

It is quite intuitive that pressure drop in helical and wavy fiber configurations would be higher than their straight counterparts. A procedure to calculate relative pressure drop and energy cost in helical geometries with respect to straight fibers has been

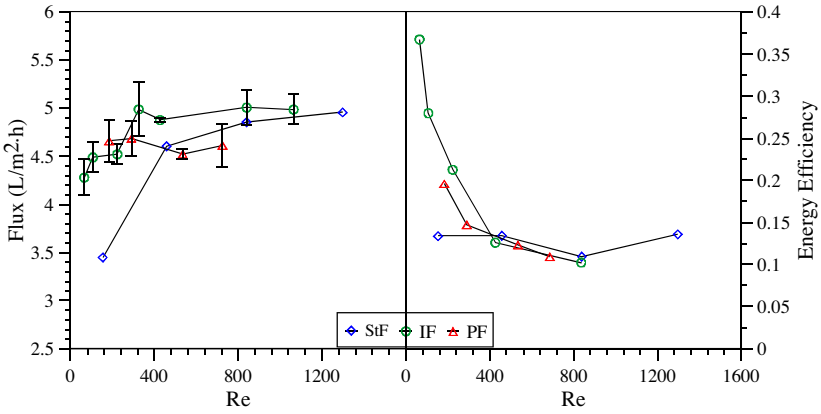

Fig. 8. Flux and energy efficiency for intermittent (IF), pulsating (PF) and steady flows (StF) under the same thermal conditions of 54 °C.

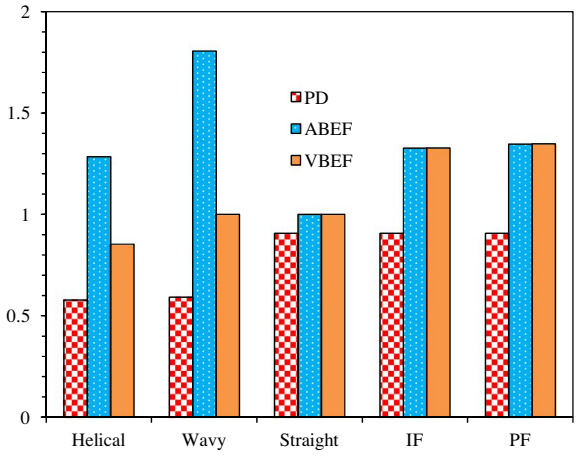

Fig. 9. Packing density (PD), area based enhancement factor (ABEF) and volume based enhancement factor (VBEF) for different configurations.

explained in Appendix. The pressure drop in wavy fibers has been assumed similar to helical ones. In spite of relatively high pressure drops, the cost associated with pumping energy per unite flux for undulating module configurations is lower than their straight counterparts. Pumping cost per unit flux for helical and wavy configurations is 17% and 22%, respectively, lower than straight fiber configurations.

3.2.2. Intermittent and pulsating flow

The experimentation was also carried out by using the flow in intermittent and pulsating mode of feed flow generated according to procedures explained in Figs. 2 and 3. *Re* calculated for pulsating flow is based on the average flow rate recorded. The flux and energy efficiency analysis for intermittent and pulsating flow have been compared with that obtained by using steady flow in Fig. 8 and show very interesting pattern. Even at very low *Re* (~76), the flux obtained for intermittent flow is significantly higher than that observed for the steady flow. The maximum difference in flux between intermittent and steady flow is 30%. The back and forth flow frequency is very low at lower flow rates but still it is effective to improve the mixing of fluid present at the membrane surface with the bulk. Moreover, due to high magnitude of backward component of flow at low frequencies, the residence time of the fluid in the module becomes high, leading towards more cooling. More increase in frequency further improves mixing and at the same time, decreases the residence time of fluid in the module. As the flow rate is increased further, the forward component of back and forth flow increases and the effectiveness of intermittent flow starts to diminish. At high *Re*, the flux behavior resembles with that of steady flow. The observed increase in flux is similar to what has been observed in other active techniques applied for membrane distillation. Chen et al. [51] has achieved an average flux enhancement of 26% by applying gas bubbling technique to reduce temperature polarization and scaling at membrane surface in DCMD. Two phase flow applied in their study, however, adds an additional complexity.

A comparison of *EE* for intermittent and pulsating flows with steady flow has also been provided in Fig. 8. It is evident from the figure that the highest *EE* is achieved for intermittent flow mode within the experimental flow conditions studied. The maximum difference observed between the *EE* for steady and intermittent flow is ~180% (even at much low *Re* of intermittent flow) and it starts to approach to that of the steady flow with increase in flow. As evident from the figure, a significantly high value of flux is achieved at very low feed flow rates for intermittent flow which causes a high *EE* for this flow pattern. *EE* for pulsatile flow follows the similar trend to that of intermittent flow. However, it was not possible to operate the system used in present study below a certain value of *Re* for pulsating flow, therefore, *EE* for pulsating flow at low *Re* has not been mentioned in the current study.

The pumping cost for both flow patterns applied has been calculated on the basis of average flow rate at module inlet according to the procedure explained in Appendix. The calculations reveal that intermittent flow has the possibility to reduce pumping cost per unit flux by ~193% as compared to steady flow. For pulsatile flow, this figure drops down to 13%. The huge reduction in pumping cost per unit flux for intermittent flow is due to the capability of this type of flow to generate high fluxes at very small average feed flow rates.

3.3. Packing density

One of the major advantages of the membrane operations is their very high surface to volume ratio dictated by the high packing density of the module. Packing density for hexagonal lattice of straight module is 90.7% [52], although very high values can negatively disturb the heat and mass transfer on the shell side. For helical and wavy configurations, packing density varies with membrane outer diameter and coil diameter of the helix. In case of helical fiber, the space present inside the helix restricts the further increase in packing density. In case of wavy fibers, for a given membrane, it is function of wave length and outer diameter of the

membrane. Packing density for different configurations has been calculated by using the modules parameters used in the current study according to the correlation provided in [52]. The packing density plays a crucial role in dictating the overall module volume which can be important for certain applications. On the other hand, an area based enhancement factor (ABEF) gives an indication of the membrane area in comparison to the straight configuration to achieve a particular separation volume [52]. ABEF affects both membrane cost and operational cost. Similarly, volume based enhancement factors (VBEF) gives an indication of the improvement in flux per unit change in module volume with respect to straight fibers.

Packing densities along with area and volume based enhancement factors for different configurations applied have been shown in Fig. 9. Obviously, the best packing density can be expected for straight module. Since the straight fibers have been used for intermittent and pulsating flow experimentation, their packing density is the same as that for the straight fibers used in steady flow. The packing densities are significantly lower for helical and wavy configurations (59% and 57%, respectively). Area based and volume based enhancement factors were calculated at Re ~230 for all flow pattern and module configurations used according to correlations used in [52]. ABEF is maximum for wavy shaped geometry which somehow indicates a lower operational and capital cost for such modules, although the low packing density and VBEF [52] are the drawback of this configuration. Similarly, EBEF for helical geometry is attractive (1.28) but packing density and VBEF are lower. Intermittent and pulsating flow modes seem to be the best optimum due to their reasonable ABEF (1.32), high packing density and VBEF, however, the additional cost associated with the realization of these flow patterns has not been considered.

4. Conclusions

The performance of MD by using traditional straight fibers and steady flow is severely affected due to temperature polarization at low feed flow rates. Various flow patterns and undulating fiber geometries used to augment heat transfer in heat exchanger applications and to reduce concentration polarization in traditional membrane processes are promising candidates to reduce thermal polarization in MD. Encouraging results have been achieved by using pure water and whey solution as feed in current study. The improvement in performance through both the techniques can be realized mainly at low feed flow rate where the system is controlled by the boundary layer resistance. This observation provides the opportunity of saving pumping energy without compromising the membrane performance. At low feed flow rates, wavy shaped fibers exhibit the highest mass transfer rate enhancement of ~52%. On the other hand, intermittent flow shows 180% improvement in energy efficiency. Experimental results indicate that intermittent flow and wavy module configuration have the potential to reduce the pumping cost per unit flux approximately by 200% and 23%, respectively than their conventional counterparts. In terms of surface and volume based enhancement factor and packing density, intermittent and pulsating flows displayed most optimal performance.

Acknowledgement

The authors acknowledge the financial support from European Commission under the project "Erasmus Mundus Joint Doctorate in Membrane Engineering (Grant number FPA 2011-0014)" to carry out the current research.

Appendix

Table A1. Correlations used for the calculation of heat transfer coefficients.

$Nu = 1.86\left(\frac{Re\ Pr}{L/D}\right)^{1/3}$	(A1)	[53]
$Nu = 4.36 + \frac{0.036 Re\ Pr(D/L)}{1+0.0011(RePr(D/L))^{0.8}}$	(A2)	[54]
$Nu_{cooling} = 11.5(Re\ Pr)^{0.23}(D/L)^{0.5}$	(A3)	[55]
$Nu_{heating} = 15(Re\ Pr)^{0.23}(D/L)^{0.5}$	(A4)	[55]
$Nu = 0.13(Re)^{0.64}(Pr)^{0.38}$	(A5)	[55]
$Nu = 1.95\left(\frac{Re\ Pr}{L/D}\right)^{1/3}$	(A6)	[56]
$Nu = 0.097(Re)^{0.73}(Pr)^{0.13}$	(A7)	[55]
$Nu = 3.66 + \frac{0.104 Re\ Pr(D/L)}{1+0.0106(Re\ Pr(D/L))^{0.8}}$	(A8)	[56]

Calculation procedure for pumping cost

Ratio of Fanning friction factor in helical and straight fibers has been calculated by the following correlation [57]:

$$f_c/f_s = \left(1 - \left[1 - \left(\frac{11.6}{De}\right)^{0.45}\right]^{0.22}\right)^{-1} \quad (A9)$$

As fanning friction factor is proportional to pressure drop, therefore for the same feed type and flow rate:

$$f_c/f_s = \Delta P_h/\Delta P_s \quad (A10)$$

On the basis of pressure drop, the relative pumping cost can be calculated according to the following correlation [58]:

$$C_{pumping} = 0.014 G_e \cdot P \quad (A11)$$

where G_e is the feed flow in kg/h rate and P is the pressure in atmosphere.

Pumping cost per unit flux for different fiber geometries and flow patterns can be calculated by dividing the pumping cost for each configuration/flow pattern with the corresponding flux. For intermittent and pulsatile flows, *Ge* is based upon the average flow rate at the module inlet while P is assumed equal to that for the steady flow.

List of symbols and abbreviations

A_m	membrane area (m^2)
B	membrane characteristic parameter
C_p	specific heat (J/kg K)
D	diameter (m)
EE	energy efficiency
f	friction factor
h_c	conductive heat transfer coefficient (W/m^2 K)
h_f	feed side heat transfer coefficient (W/m^2 K)
h_p	permeate side heat transfer coefficient (W/m^2 K)
h_v	vapor heat transfer coefficient of membrane (W/m^2 K)
J	flux (kg/m^2 h)
K	thermal conductivity (W/m K)
M	molecular weight (kg/mol)
Nu	Nusselt number
P	vapor pressure (Pa)
Pr	Prandtl number

(*continued on next page*)

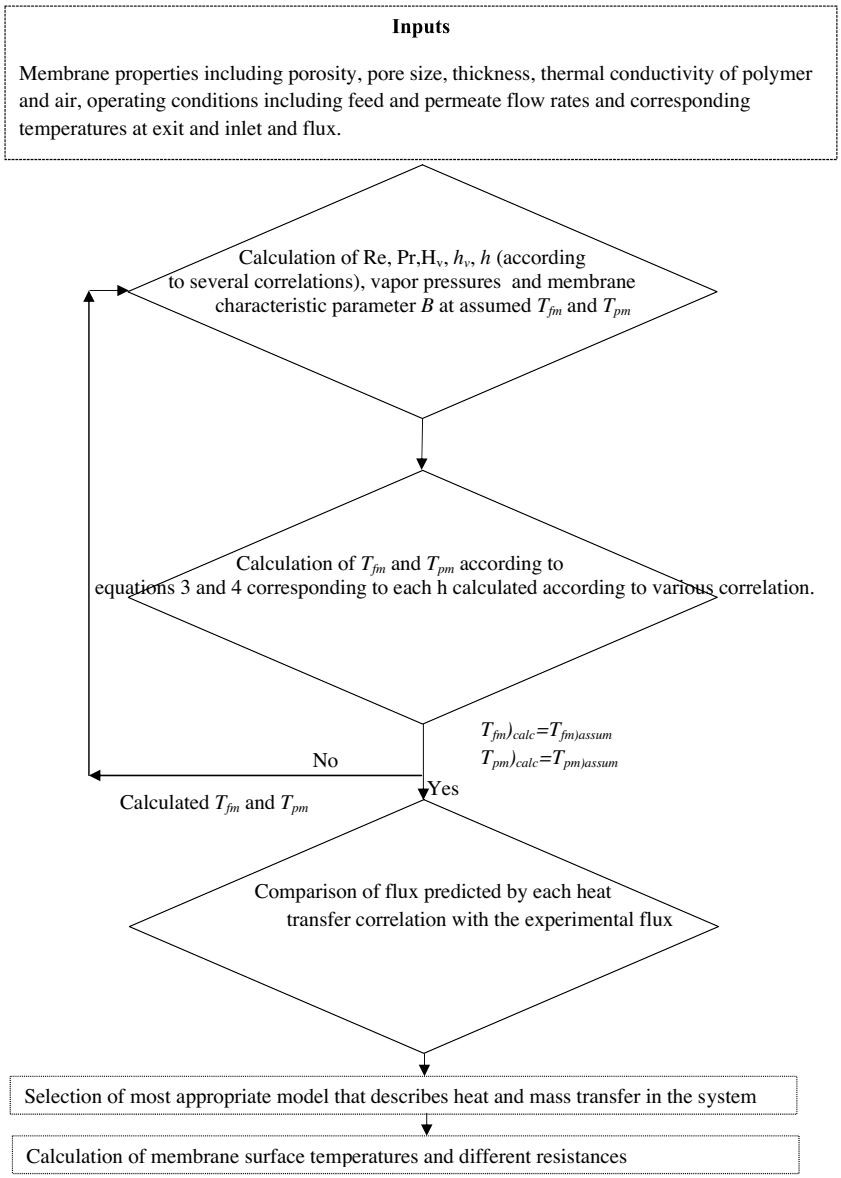

Fig. A1. Algorithm used to calculate the most suitable heat transfer correlation for membrane used and various resistances.

R	universal gas constant (J/K mol)
Re	Reynolds number
T	temperature (K)
δ	membrane thickness (m)
τ	tortuosity factor
ε	porosity
μ	viscosity (Pa s)

References

[1] E. Drioli, A. Ali, F. Macedonio, Membrane distillation: recent developments and perspectives, Desalination 356 (2015) 56–84.

[2] L. Francis, N. Ghaffour, A.A. Alsaadi, G.L. Amy, Material gap membrane distillation: a new design for water vapor flux enhancement, J. Membr. Sci. 448 (2013) 240–247.

[3] K. Zhao, W. Heinzl, M. Wenzel, S. Büttner, F. Bollen, G. Lange, S. Heinzl, N. Sarda, Experimental study of the memsys vacuum-multi-effect-membrane-distillation (V-MEMD) module, Desalination 323 (2013) 150–160.

[4] D. Winter, J. Koschikowski, S. Ripperger, Desalination using membrane distillation: flux enhancement by feed water deaeration on spiral-wound modules, J. Membr. Sci. 423–424 (2012) 215–224.

[5] A. Ali, F. Macedonio, E. Drioli, S. Aljlil, O.A. Alharbi, Experimental and theoretical evaluation of temperature polarization phenomenon in direct contact membrane distillation, Chem. Eng. Res. Des. 91 (10) (2013) 1966–1977.

[6] K.W. Lawson, D.R. Lloyd, Membrane distillation, J. Membr. Sci. 124 (1997).

[7] R.W. Schofield, A.G. Fane, Heat and mass transfer in membrane distillation, J. Membr. Sci. 33 (1987) 299–313.

[8] J. Phattaranawik, R. Jiraratananon, A. Fane, Heat transport and membrane distillation coefficients in direct contact membrane distillation, J. Membr. Sci. 212 (1–2) (2003) 177–193.

[9] M. Gryta, Concentration of saline wastewater from the production of heparin, Desalination 129 (2000) 35–44.

[10] A. Kullab, A. Martin, Membrane distillation and applications for water purification in thermal cogeneration plants, Sep. Purif. Technol. 76 (3) (2011) 231–237.

[11] M. Gryta, Direct contact membrane distillation with crystallization applied to NaCl solutions, in: Chemical Paper, 2002, 56 (May 2001) 14–19.

[12] A. Hausmann, P. Sanciolo, T. Vasiljevic, M. Weeks, K. Schroën, S. Gray, M. Duke, Fouling mechanisms of dairy streams during membrane distillation, J. Membr. Sci. 441 (2013) 102–111.

[13] M.Y. Jaffrin, Hydrodynamic techniques to enhance membrane filtration, Annu. Rev. Fluid Mech. 44 (77–96) (2012).

[14] R. Moll, D. Veyret, F. Charbit, P. Moulin, Dean vortices applied to membrane process, J. Membr. Sci. 288 (1–2) (2007) 307–320.

[15] S. Luque, H. Mallubhotla, G. Gehlert, R. Kuriyel, S. Dzengeleski, S. Pearl, G. Belfort, A new coiled hollow-fiber module design for enhanced microfiltration performance in biotechnology, Biotechnol. Bioeng. 65 (3) (1999) 247–257.

[16] P. Naphon, S. Wongwises, A review of flow and heat transfer characteristics in curved tubes, Renew. Sust. Energy Rev. 10 (5) (2006) 463–490.

[17] X. Yang, R. Wang, A.G. Fane, Novel designs for improving the performance of hollow fiber membrane distillation modules, J. Membr. Sci. 384 (1–2) (2011) 52–62.
[18] K.M. Lim, J.Y. Park, J.C. Lee, J.C. Kim, B.G. Min, E.T. Kang, E.B. Shim, Quantitative analysis of pulsatile flow contribution to ultrafiltration, Artif. Organs 33 (1) (2009) 69–73.
[19] N.W. Zulkifli, Experimental study of pulsatile flows in a heated horizontal tube for various flow ρ, in: ICET07, 2007, pp. 11–13.
[20] C. Huang, H.-S. Chen, The characteristic analysis of interrupted flow pulsation on ultrafiltration system, Appl. Mech. Mater. 479–480 (2014) 373–379.
[21] G. Chen, X. Yang, R. Wang, A.G. Fane, Performance enhancement and scaling control with gas bubbling in direct contact membrane distillation, Desalination 308 (2013) 47–55.
[22] Z. Ding, L. Liu, Z. Liu, R. Ma, The use of intermittent gas bubbling to control membrane fouling in concentrating TCM extract by membrane distillation, J. Membr. Sci. 372 (1–2) (2011) 172–181.
[23] K. Katsoufidou, S.G. Yiantsios, A.J. Karabelas, An experimental study of UF membrane fouling by humic acid and sodium alginate solutions: the effect of backwashing on flux recovery, Desalination 220 (2008) 214–227.
[24] J. Wu, P. Le-clech, R.M. Stuetz, A.G. Fane, V. Chen, Effects of relaxation and backwashing conditions on fouling in membrane bioreactor, J. Membr. Sci. 324 (2008) 26–32.
[25] C. Bhattacharjee, P.K. Bhattacharya, Ultrafiltration of black liquor using rotating disk membrane module, Sep. Purif. Technol. 49 (2006) 281–290.
[26] L.M. Vane, F.R. Alvarez, E.L. Giroux, Reduction of concentration polarization in pervaporation using vibrating membrane module, J. Membr. Sci. 153 (1999) 233–241.
[27] W.R. Dean, The stream-line motion of fluid in a curved pipe, Philos. Mag. Ser. 7 5 (30) (1928) 673–695.
[28] M.E. Brewster, K. Chung, G. Belfort, Dean vortices with wall flux in a curved channel membrane system: a new approach to membrane module design, J. Membr. Sci. 81 (1993) 127–137.
[29] P. Moulin, J.C. Rouch, C. Serra, M.J. Clifton, P. Aptel, Mass transfer improvement by secondary flows: Dean vortices in coiled tubular membranes, J. Membr. Sci. 114 (2) (1996) 235–244.
[30] P. Moulin, P. Manno, J.C. Rouch, C. Serra, M.J. Clifton, P. Aptel, Flux improvement by Dean vortices: ultrafiltration of colloidal suspensions and macromolecular solutions, J. Membr. Sci. 156 (1999) 109–130.
[31] P. Manno, J.C. Rouch, M. Clifton, P. Aptel, Mass transfer improvement in helically wound hollow fibre ultrafiltration modules yeast suspensions, Sep. Purif. Technol. 14 (1998) 175–182.
[32] H. Mallubhotla, S. Hoffmann, M. Schmidt, J. Vente, G. Belfort, Flux enhancement during dean vortex tubular membrane nanofiltration, J. Membr. Sci. 141 (1998) 183–195.
[33] B.Y.J.R. Lines, F. Path, Helically Coiled Heat Exchangers Offer Advantages, Graham Man, no. September. pp. 1–5, 1991. Available online at <www.graham-mfg.com/usr/pdf/techlibheattransfer/14.pdf>.
[34] P. Coronel, K.P. Sandeep, Heat transfer coefficient in helical heat exchangers under turbulent flow conditions, Int. J. Food Eng. 4 (1) (2008).
[35] A.M. Elsayed, Heat Transfer in Helically Coiled Small Diameter Tubes for Miniature Cooling Systems, University of Birmingham Edgbaston, Birmingham, B15 2TT, 2011.
[36] M.M. Teoh, S. Bonyadi, T. Chung, Investigation of different hollow fiber module designs for flux enhancement in the membrane distillation process, J. Membr. Sci. 311 (2008) 371–379.
[37] K. Tatebe, M. Yamazaki, Oxygenator using porous hollow fiber membrane, US 54893821996.
[38] T. Taniguchi, N. Suga, T. Otoyo, United States Patent, Method for purifying aqueous suspension, 6495041 B22002.
[39] C. Zhu, G.L. Liu, C.S. Cheung, C.W. Leung, Z.C. Zhu, Ultrasonic stimulation on enhancement of air gap membrane distillation, J. Membr. Sci. 161 (1999) 85–93.
[40] C. Zhu, G. Liu, Modeling of ultrasonic enhancement on membrane distillation, J. Membr. Sci. 176 (January) (2000) 31–41.
[41] Karl E. Karlson, Ronald J. Massimino, Arun K. Singh, George N. Cooper, Jr., Laboratory and clinical evaluation of a membrane oxygenator with secondary flows in the blood channels, World J. Surg. 6 (1982) 358–361.
[42] M.-A. Hessami, N. W. Zulfiki, Experimental study of pulsatile flows in a heated horizontal tube for various flow ρ, in: ICET07, 2007, pp. 11–13.
[43] K.M. Lim, E.B. Shim, Computational assessment of the effects of a pulsatile pump on toxin removal in blood purification, Biomed. Eng. Online 31 (2010) 1–16.
[44] A. Faghri, M. Faghri, K. Javdani, Effect of flow pulsation on laminar heat transfer between two parallel plates, Warme- und Stoffiibertragung 13 (1980) 97–103.
[45] Z. Guo, S.Y. Kim, H.J. Sung, Pulsating flow and heat transfer in a pipe partially filled with a porous medium, Int. J. Heat Mass Transf. 40 (17) (1997) 4209–4218.
[46] M. Jafari, M. Farhadi, K. Sedighi, Pulsating fl ow effects on convection heat transfer in a corrugated channel: a LBM approach, Int. Commun. Heat Mass Transf. 45 (2013) 146–154.
[47] A. Hausmann, P. Sanciolo, T. Vasiljevic, M. Weeks, K. Schroën, S. Gray, M. Duke, Fouling of dairy components on hydrophobic polytetrafluoroethylene (PTFE) membranes for membrane distillation, J. Membr. Sci. 442 (2013) 149–159.
[48] P. Wang, T. Chung, Design and fabrication of lotus-root-like multi-bore hollow fiber membrane for direct contact membrane distillation, J. Membr. Sci. 421–422 (2012) 361–374.
[49] D.N. Kuakuvi, P. Moulin, F. Charbit, Dean vortices: a comparison of woven versus helical and straight hollow fiber membrane modules, J. Membr. Sci. 171 (1) (2000) 59–65.
[50] A. Hausmann, P. Sanciolo, T. Vasiljevic, U. Kulozik, M. Duke, Performance assessment of membrane distillation for skim milk and whey processing, J. Dairy Sci. 97 (1) (2014) 56–71.
[51] G. Chen, X. Yang, R. Wang, A.G. Fane, Performance enhancement and scaling control with gas bubbling in direct contact membrane distillation, Desalination 308 (2013) 47–55.
[52] D. Kaufhold, F. Kopf, C. Wolff, S. Beutel, L. Hilterhaus, M. Hoffmann, Generation of Dean vortices and enhancement of oxygen transfer rates in membrane contactors for different hollow fiber geometries, J. Membr. Sci. 424 (2012) 342–347.
[53] E.N. Sieder, G.E. Tate, Heat transfer and pressure drop of liquids in tubes, Ind. Eng. Chem. 28 (1936) 1429–1435.
[54] M. Gryta, M. Tomaszewska, Heat transport in the membrane distillation process, J. Membr. Sci. 144 (February) (1998).
[55] M. Gryta, M. Tomaszewska, A.W. Morawski, Membrane distillation with laminar flow, Sep. Purif. Technol. 5866 (97) (1997) 2–6.
[56] L.C. Thomas, Heat Transfer, Prentice-Hall, Englewood Cliffs, NJ, 1992.
[57] C.M. White, Fluid friction and its relation to heat transfer, Trans. Inst. Chem. Eng. 10 (1932) 66–86.
[58] A.M. Helal, A.M. El-Nashar, E. Al-Khateeri, S. Al-Malek, Optimal design of hybrid RO/MSF desalination plants. Part I: Modeling and algorithms, Desalination 154 (2003) 43–66.